

324-fs Pulses From a SESAM Modelocked Backside-Cooled 2- μm VECSEL

Jonas Heidrich¹, Marco Gaulke¹, Matthias Golling¹, Behcet Ozgur Alaydin¹,
Ajanta Barh¹, and Ursula Keller¹, *Fellow, IEEE*

Abstract—We present the first modelocked backside-cooled GaSb VECSEL (Vertical External Cavity Surface Emitting Laser) operating above 2 μm . Using a two quantum well InGaSb SESAM (Semiconductor Saturable Absorber Mirror) in a V-shaped cavity arrangement we obtain femtosecond modelocking at a center wavelength of 2061 nm, with pulses as short as 324 fs, an average output power as high as 65 mW at a repetition rate of 3 GHz. An operation in a picosecond regime is further demonstrated with an even higher average output power of up to 260 mW and 4.5-ps pulses. We perform a characterization in both the femto- and picosecond regimes with measurements of the pulse duration, the optical spectrum, and the pulse repetition rate (frequency and time domain analysis) at low and high power. In this context, the influence of intracavity group delay dispersion (GDD) is investigated. We find that GDD has a strong influence on the pulse duration (fs or ps regime) and thus on the performance of our SESAM-modelocked 2- μm GaSb VECSEL.

Index Terms—GaSb, VECSEL, SESAM, semiconductor lasers, modelocking, infrared ultrafast laser, optical frequency comb.

I. INTRODUCTION

THE optically pumped SESAM-modelocked vertical external cavity surface emitting laser (VECSEL) [1] combines excellent beam quality, high average power, and wavelength versatility together with high repetition rates and compact cavity design. So far, mainly GaAs and InP III-V semiconductor-based VECSELs are explored for ultrashort pulse generation, working from the visible up to 1.6 μm wavelength [2]–[4]. A strong demand for high-speed and precise molecular spectroscopy applications has recently increased the interest in modelocked lasers operating beyond 2 μm . The preferred material system for VECSELs in this spectral region is GaSb. Such VECSELs have been investigated for more than a decade, but outstanding results were only achieved in continuous wave (cw) operation using an intracavity, top heat spreader [5], [6]. Modelocking of a top-cooled VECSEL using a semiconductor saturable absorber mirror (SESAM) has also been demonstrated, however with limited output power at

Manuscript received January 17, 2022; revised February 23, 2022; accepted February 25, 2022. Date of publication March 2, 2022; date of current version March 11, 2022. This work was supported by the European Research Council (ERC) under the European Union’s Horizon 2020 Research and Innovation Program under Grant 787097. (Corresponding author: Jonas Heidrich.)

The authors are with the Ultrafast Laser Physics Group, Institute for Quantum Electronics, ETH Zürich, 8093 Zürich, Switzerland (e-mail: hejonas@phys.ethz.ch).

Color versions of one or more figures in this letter are available at <https://doi.org/10.1109/LPT.2022.3156181>.

Digital Object Identifier 10.1109/LPT.2022.3156181

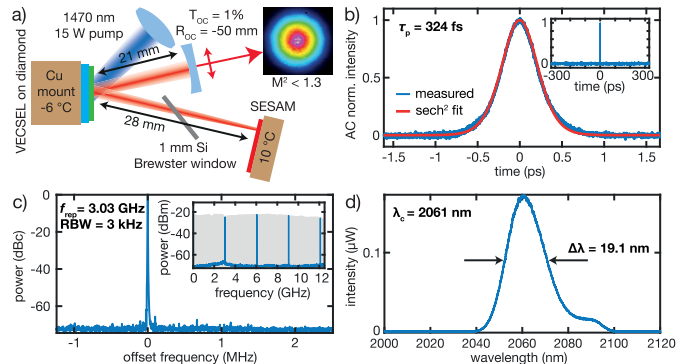


Fig. 1. Cavity and modelocking diagnostics. a) V-shaped VECSEL cavity. The VECSEL serves as double pass gain and folding mirror. A 1% output coupler (OC) with -50 mm radius of curvature and a SESAM serve as cavity end mirrors. b) Autocorrelation measurement of the shortest pulse configuration (blue) together with a sech^2 fit with a 324-fs FWHM pulse duration (red). Inset: wide scan intensity autocorrelation of $>\pm 250$ ps showing no side pulses. c) Microwave spectrum of the pulse repetition rate peak at 3 GHz sampled with a resolution bandwidth (RBW) of 3 kHz indicates clean modelocking. Inset: large span of the microwave spectrum (RBW 100 kHz) showing the presence of higher harmonics of the repetition rate with equal spectral power referenced to the microwave spectrum analyzer response (grey area). d) Measured optical spectrum of the laser pulse. The spectrum is centered at 2061 nm with a FWHM bandwidth $\Delta\lambda$ of 19.1 nm.

a repetition rate below 1 GHz and emission wavelength in the atmospheric water absorption band near 2 μm [7].

We present the first modelocked GaSb-VECSEL without any intracavity heat spreader [8] and operating at 2061 nm, far from atmospheric water absorption. An InGaSb quantum well SESAM is used for passive modelocking [9]. The compact laser cavity delivers pulses as short as 324 fs at a repetition rate of 3 GHz. The average output power is 38 mW, which can be increased to 65 mW by increasing the pump power. We have achieved a fourfold improved efficiency of 1.3% ($P_{\text{out}}/P_{\text{in}}$), compared to previous results [7]. Furthermore, the cavity can be operated in a picosecond (ps) modelocking regime with an average output power of up to 260 mW. On a long-term timescale of more than 20 minutes, the rms power fluctuation is below 0.15%. The two different pulse-duration regimes can be obtained with a tunable intracavity roundtrip group delay dispersion (GDD) as described here.

II. VECSEL CAVITY DESIGN

The modelocked VECSEL cavity consists of four elements: a VECSEL gain mirror, a SESAM, a curved output coupler (OC) and a 1-mm silicon (Si) window (Fig. 1a).

The VECSEL chip consists of 15 $\text{In}_{0.27}\text{Ga}_{0.73}\text{Sb}$ quantum wells (QW) with a thickness of 8 nm placed around the peak of the standing-wave profile grown on top of a 19.5 pair $\text{GaSb}/\text{AlAs}_{0.08}\text{Sb}_{0.92}$ distributed Bragg reflector (DBR). This VECSEL gain chip was grown at ETH Zurich in reverse order using molecular beam epitaxy (MBE). Afterwards the gain chip is vacuum soldered to a $5 \times 5 \text{ mm}^2$ diamond heat sink prior to the GaSb-wafer removal, which enables backside-cooling of the gain structure via the diamond heat sink [10]. This has the advantage that no intracavity heat spreader is needed which avoids additional losses and an undesired intracavity etalon. A $\lambda/4$ Si_3N_4 antireflection coating grown by plasma enhanced chemical vapor deposition (PECVD) is applied for an enhanced field intensity in the active region and thus to increase the gain, enabling high-power cw operation. The optical characterization of the chip under intracavity lasing conditions show a broad gain bandwidth of more than 90 nm, a small signal gain of $\sim 5\%$, and a saturation fluence of $2 \mu\text{J}/\text{cm}^2$ measured with 100-fs pulses. The saturation fluence is especially important for the quasi-soliton pulse shaping mechanism in modelocked VECSELs [11]. A detailed description of the structure design, the wafer removal process, and chip characterization is given in [12]. The $\text{In}_{0.27}\text{Ga}_{0.73}\text{Sb}$ QW SESAM is also MBE grown and directly soldered (GaSb wafer side) to a copper heat sink. A single layer Si_3N_4 PECVD coating with a thickness of $1.8 \mu\text{m}$ is applied which increases the electric field intensity in the two 11-nm thick saturable absorber QWs and enables a near-zero and flat cavity roundtrip GDD at the lasing wavelength. Ellipsometry characterization of the coating reveals a center to edge thickness variation of ~ 60 nm to tune the GDD. The SESAM structure is optimized for low saturation fluence of $1.3 \mu\text{J}/\text{cm}^2$, low nonsaturable losses $< 0.2\%$ and a modulation depth of up to 2% (slightly depending on the SESAM position). The fast recovery of the SESAM within 20 ps is ideal for passive modelocking of high-repetition rate VECSELs. This is attributed to recombination channels via trap states in strained InGaSb QWs and enhanced by Auger recombination due to high carrier densities generated by the incident pulse in the low bandgap QW material. All SESAM parameters have been measured with our optical SESAM characterization setups using 100-fs pulses [9]. The OC has an ion beam sputtered coating with a transmission of 1% and flat zero GDD around 2060 nm.

Our 49-mm long V-cavity is optically pumped under 45° by a 1470-nm 15-W diode laser bar focused onto the VECSEL chip to obtain a round spot of 360- μm diameter using beam-shaping with two cylindrical lenses of different focal lengths. A radius of curvature of -50 mm of the OC scales the intracavity mode sizes (diameter) to 280 μm on the VECSEL chip and 65 μm on the SESAM to obtain a fluence ratio of ~ 15 between SESAM and VECSEL. This enables dynamic gain saturation with the SESAM saturating before the VECSEL gain chip. The emission and absorption spectrum of VECSEL chip and SESAM are optimized by thermoelectrically temperature stabilizing the chips to -6°C and 10°C , respectively. The VECSEL chip temperature is chosen such that a high output power is obtained while condensation of humidity is effectively prevented with a gentle nitrogen flow. We use an

additional 1-mm thick uncoated Si Brewster window inside the cavity to introduce required positive GDD and to obtain a purely p -polarized output. For transform limited pulse generation a slightly positive cavity roundtrip GDD is required [11]. The GDD control of our cavity is discussed in section IV. The described configuration generates a high-quality Gaussian output beam, measured using an infrared bolometer camera (inset in Fig. 1a), with an $M^2 < 1.3$ at all output powers, measured using an extended InGaAs scanning slit profiler and a linear stage.

III. MODELOCKING PERFORMANCE

For the pulse characterization we use an intensity auto-correlator (AC), an optical spectrum analyzer (OSA), and a 25-dB amplified 12.5-GHz extended InGaAs fast photodiode (PD) which is either connected to a microwave spectrum analyzer (MSA) or a fast 33-GHz oscilloscope. The shortest 324-fs pulses achieved at an average output power of 38 mW with 4.2 W of pump power are shown in Fig. 1b – d. This has been the shortest pulse reported from a modelocked GaSb-VECSEL so far. A zoomed out ± 250 ps wide scan shows the absence of side pulses (Fig. 1b). From the MSA spectrum we obtain a sharp peak with a high signal to noise ratio > 65 dB at the repetition frequency of 3 GHz confirming fundamental modelocking. A large span MSA trace ranging from 0 Hz to 12.5 GHz exhibits all higher harmonics of the fundamental pulse repetition rate with equal power referenced to the MSA's electronic response (Fig. 1c). The optical spectrum is centered around 2061 nm with a full width at half maximum (FWHM) bandwidth of 19.1 nm indicating close to transform limited pulses with 1.41 times the time-bandwidth product (TBP) of a transform limited sech^2 pulse shape (Fig. 1d)

The output power as a function of pump power in the fs-regime is investigated (Fig. 2a). We find the typical hysteresis behavior of modelocked lasers and a maximum power of 65 mW. At this power level clean modelocking is maintained and a pulse broadening to 415 fs is observed together with a small spectral red shift of the center wavelength to 2069 nm. This happens due to stronger pumping and the related temperature rise in the QW gain region. We assume that the shift of the lasing wavelength for higher pump powers (Fig. 3b) moves the gain spectrum out of the optimal balanced GDD regime and thus causes broadened pulses, which is in contrast to established models [13] and is under further investigation.

The modelocked output power can be increased up to 260 mW when operating the VECSEL cavity in a ps-regime (Fig. 2c). We measure pulse durations from 2.34 ps at 72 mW up to 4.52 ps at 260 mW (Fig. 2d and e). The insets show the corresponding optical spectra revealing a larger spectral shift from 2053 nm to 2073 nm due to the stronger pumping with a power from 4.3 W up to 9.8 W. The spectral shift of the VECSEL is caused by heat deposition on the gain chip under pumping conditions and is typically a few nanometers per watt pump power. The temperature induced SESAM QW shift is estimated to have the same magnitude and happens due to absorbed intracavity power when modulating the SESAM. The asymmetric shape of the spectrum at high power is discussed in the next section. We observe a small coherence spike in

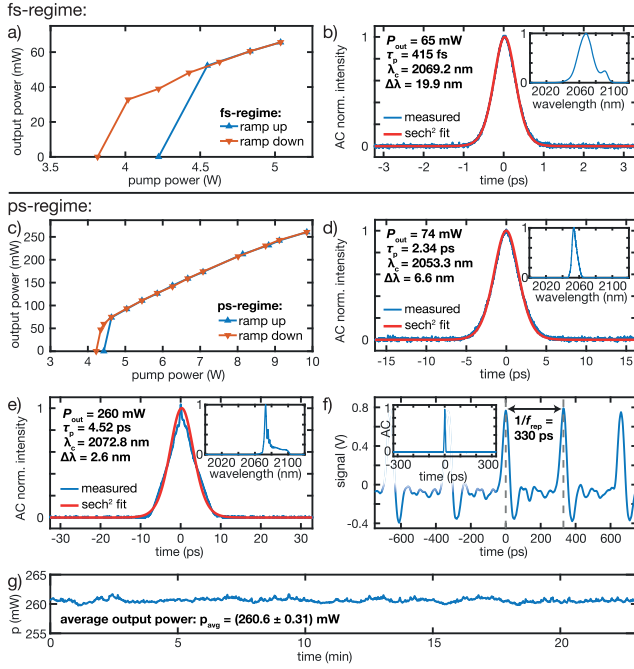


Fig. 2. Femtosecond and picosecond regime. a) Output power as a function of pump power in the fs-regime. Ramping up and down the pump power exhibits a hysteresis in output power which is typical for modelocking. b) Autocorrelation measurement (blue) and sech^2 fit (red) for the highest output power of 65 mW in the fs-regime. c) Output power as a function of pump power in the ps-regime. The maximum average output power is 260 mW showing hysteresis as well. d) & e) Autocorrelation measurement (blue) and sech^2 fit (red) for the output power of 74 mW and 260 mW in the ps-regime, respectively. Insets: corresponding normalized optical spectrum. Center wavelength λ_c , optical bandwidth $\Delta\lambda$, and pulse duration τ_p are given. f) Fast oscilloscope trace of the modelocked pulse train at highest power of 260 mW. Inset: wide scan autocorrelation showing clean fundamental modelocking at highest power. The oscilloscope time trace validates the absence of double pulses outside the ± 250 ps scan range of the autocorrelator. g) Power stability measurement at highest power. The average output power over more than 20 minutes shows rms fluctuations less than 0.15%.

the AC trace at highest power (Fig. 2e) which can indicate modelocking instabilities [14], a time-trace recorded using the 12.5-GHz photodiode connected to a 33-GHz oscilloscope is shown in Fig. 2f together with a wide scan autocorrelation trace (inset). These sanity check measurements confirm the absence of any side pulses even at highest average output power.

In order to demonstrate the laser stability, a 20-minute power measurement at highest output power of 260 mW is performed and shown in Fig. 2g. The standard deviation of this measurement reveals low fluctuations of maximum ± 0.31 mW corresponding to less than 0.15%. No drift of the output power is observed.

IV. GDD TUNING FOR TWO MODELOCKING REGIMES

Fundamental modelocking in an ultrashort fs-regime and in a ps-regime with high output power is demonstrated. We attribute the two regimes to a different amount of positive intracavity roundtrip GDD which is validated by simulations. Fig. 3a shows the spectral contributions which add up to the cavity roundtrip GDD. A pulse travelling in the cavity has two passes on the VECSEL, two passes through the Si Brewster window, and one reflection at the SESAM end mirror.

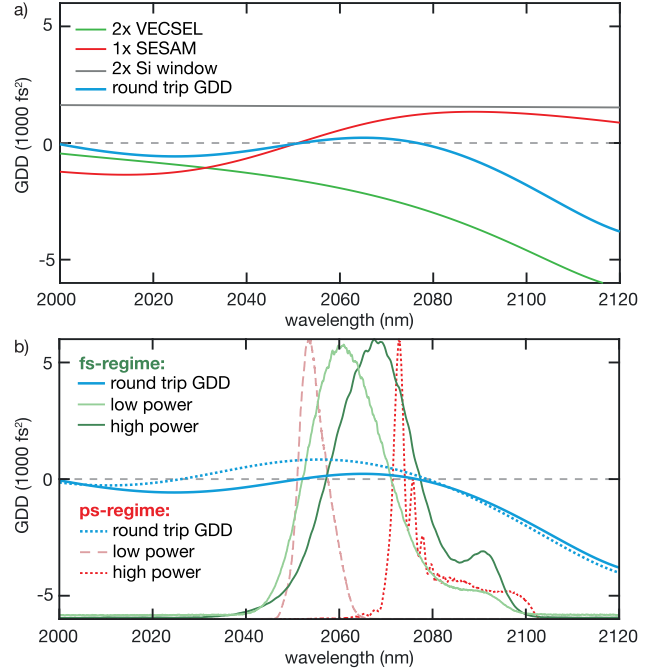


Fig. 3. Simulated intracavity GDD as a function of wavelength. a) Significant contributions to the cavity roundtrip GDD. A circulating pulse passes the VECSEL (green) and the silicon window (grey) twice. All contributions are added to obtain the roundtrip GDD (blue). The output coupler is designed for flat zero dispersion over this spectral region. b) Cavity roundtrip GDD of the fs-regime (blue solid) and ps-regime (blue dotted). For reference the optical spectra for low and high power in both regimes are shown.

The flat zero GDD contribution of the OC is negligible and hence not shown here. The cavity roundtrip GDD for both the fs-regime and the ps-regime is shown in Fig. 3b together with the corresponding spectra for low and high-power operation. Both regimes can continuously be accessed by simply tuning the lateral position of the SESAM keeping all other cavity elements unaltered. The change in intracavity GDD is introduced by a ~ 60 nm center to edge thickness variation of the 1.8 μm SESAM top coating. Such thickness variation is typical for PECVD coatings and has been measured using an ellipsometer.

When placing the cavity laser mode closer to the edge of the SESAM, where the top coating is slightly thicker compared to the center, the cavity can be operated in the fs-regime (Fig. 3b blue solid line) with a near-zero intracavity GDD between 2052 and 2077 nm. It is observed that the 19-nm FWHM optical spectrum is exactly located within this wavelength range (see spectra in Fig. 3b). However, there is a tradeoff between the GDD being close to zero and the scaling of the output power. The output power in clean modelocking operation is limited, as the operating wavelength is red-shifted at higher pump power and thus moves the emission wavelength out of the optimal GDD regime [11]. The operation close to the optimal GDD is confirmed by observing slightly chirped pulses. This also explains the slight increase in TBP from 1.4 to $1.8 \times$ TBP of a transform limited sech^2 pulse, while going from lowest to highest output power.

The ps-regime operation is reached when the laser cavity mode is placed at the center of the SESAM where we assume a coating thickness close to the designed thickness of 1.8 μm .

In this case, the VECSEL cavity has a net positive GDD up to $+800 \text{ fs}^2$ over a broad wavelength range from 2026 to 2079 nm (Fig. 3b blue dotted line). This results in strongly chirped pulses up to $15.3 \times \text{TBP}$ of a transform limited sech^2 with an increase of average output power up to 260 mW. The broader positive GDD bandwidth enables the spectrum to shift over 16 nm limited by the VECSEL gain on the short wavelength side and by negative GDD on the long wavelength side. This results in a strongly asymmetric spectrum.

V. CONCLUSION

We demonstrated the first modelocked VECSEL operating in the wavelength region slightly above $2 \mu\text{m}$ and show its record high performance with ultrashort pulses of 324 fs at a repetition rate of 3 GHz. Stable SESAM-modelocking in the femtosecond regime is possible with even higher average output power of up to 65 mW.

Higher average power of up to 260 mW is achieved operating the cavity in a ps-regime which can be interesting for example for medical applications. Chirped pulses ranging from 2.34 ps up to 4.52 ps with increasing power can be obtained with the same cavity adjusting the intracavity GDD. The strong influence of the GDD on parameters such as pulse duration and output power in different modelocking regimes is discussed and supported with dispersion simulations. This is in contrast to previous results stating a small dependence on intracavity GDD [7].

Our results demonstrate the high potential and versatility of backside-cooled SESAM-modelocked VECSELs in the longer wavelength regime of around $2\text{-}\mu\text{m}$. We have demonstrated power levels suitable for many applications such as optical ranging in a low absorption window [15] or spectroscopy of e.g., CO_2 at 2050 nm [16]. Future work focuses on GDD optimized VECSELs enabling further power scaling maintaining femtosecond operation. Our ultimate goal is to move from a design using a VECSEL with a SESAM in V-shaped cavities to a more integrated GaSb-MIXSEL (modelocked integrated external cavity surface emitting laser) [17] which will lead to an extremely versatile laser source emitting directly in the interesting wavelength region above $2 \mu\text{m}$.

ACKNOWLEDGMENT

The authors would like to thank Dr. V. Wittwer of University of Neuchâtel for providing the IBS coating on the output coupler and the characterization of their PECVD coating materials and also would like to thank the FIRST clean room facility of ETH Zürich.

REFERENCES

- [1] S. Hoogland *et al.*, "Passively mode-locked diode-pumped surface-emitting semiconductor laser," *IEEE Photon. Technol. Lett.*, vol. 12, no. 9, pp. 1135–1137, Sep. 2000, doi: [10.1109/68.874213](https://doi.org/10.1109/68.874213).
- [2] U. Keller and A. C. Tropper, "Passively modelocked surface-emitting semiconductor lasers," *Phys. Rep.*, vol. 429, no. 2, pp. 67–120, Jun. 2006, doi: [10.1016/j.physrep.2006.03.004](https://doi.org/10.1016/j.physrep.2006.03.004).
- [3] B. W. Tilma *et al.*, "Recent advances in ultrafast semiconductor disk lasers," *Light, Sci. Appl.*, vol. 4, no. 7, pp. 310–324, Jul. 2015, doi: [10.1038/lsa.2015.83](https://doi.org/10.1038/lsa.2015.83).
- [4] M. Guina, A. Rantamäki, and A. Härkönen, "Optically pumped VECSELs: Review of technology and progress," *J. Phys. D, Appl. Phys.*, vol. 50, no. 38, Sep. 2017, Art. no. 383001, doi: [10.1088/1361-6463/aa7bfd](https://doi.org/10.1088/1361-6463/aa7bfd).
- [5] P. Holl *et al.*, "GaSb-based $2.0 \mu\text{m}$ SDL with 17 W output power at 20°C ," *Electron. Lett.*, vol. 52, no. 21, pp. 1794–1795, Oct. 2016, doi: [10.1049/el.2016.2412](https://doi.org/10.1049/el.2016.2412).
- [6] M. Rattunde, P. Holl, and J. Wagner, "Single-frequency and high power operation of 2–3 micron VECSEL," in *Vertical External Cavity Surface Emitting Lasers*. Hoboken, NJ, USA: Wiley, 2021, pp. 63–107.
- [7] A. Haärkönen *et al.*, "Modelocked GaSb disk laser producing 384 fs pulses at $2 \mu\text{m}$ wavelength," *Electron. Lett.*, vol. 47, no. 7, p. 454, 2011, doi: [10.1049/el.2011.0253](https://doi.org/10.1049/el.2011.0253).
- [8] M. Kuznetsov, F. Hakimi, R. Sprague, and A. Mooradian, "High-power ($>0.5\text{-W}$ CW) diode-pumped vertical-external-cavity surface-emitting semiconductor lasers with circular TEM 00 beams," *IEEE Photon. Technol. Lett.*, vol. 9, no. 8, pp. 1063–1065, Aug. 1997, doi: [10.1109/68.605500](https://doi.org/10.1109/68.605500).
- [9] J. Heidrich, M. Gaulke, B. O. Alaydin, M. Golling, A. Barh, and U. Keller, "Full optical SESAM characterization methods in the 19 to $3\text{-}\mu\text{m}$ wavelength regime," *Opt. Exp.*, vol. 29, no. 5, p. 6647, Mar. 2021, doi: [10.1364/OE.418336](https://doi.org/10.1364/OE.418336).
- [10] R. Häring, R. Paschotta, A. Aschwanden, E. Gini, F. Morier-Genoud, and U. Keller, "High-power passively mode-locked semiconductor lasers," *IEEE J. Quantum Electron.*, vol. 38, no. 9, pp. 1268–1275, Sep. 2002, doi: [10.1109/JQE.2002.802111](https://doi.org/10.1109/JQE.2002.802111).
- [11] R. Paschotta, R. Häring, A. Garnache, S. Hoogland, A. C. Tropper, and U. Keller, "Soliton-like pulse-shaping mechanism in passively mode-locked surface-emitting semiconductor lasers," *Appl. Phys. B: Lasers Opt.*, vol. 75, nos. 4–5, pp. 445–451, Oct. 2002, doi: [10.1007/s00340-002-1014-5](https://doi.org/10.1007/s00340-002-1014-5).
- [12] M. Gaulke, J. Heidrich, B. Özgür Alaydin, M. Golling, A. Barh, and U. Keller, "High average output power from a backside-cooled $2\text{-}\mu\text{m}$ InGaSb VECSEL with full gain characterization," *Opt. Exp.*, vol. 29, no. 24, p. 40360, Nov. 2021, doi: [10.1364/OE.438157](https://doi.org/10.1364/OE.438157).
- [13] O. Sieber *et al.*, "Experimentally verified pulse formation model for high-power femtosecond VECSELs," *Appl. Phys. B, Lasers Opt.*, vol. 113, no. 1, pp. 133–145, 2013, doi: [10.1007/s00340-013-5449-7](https://doi.org/10.1007/s00340-013-5449-7).
- [14] D. J. Kane *et al.*, "Characteristics and instabilities of mode-locked quantum-dot diode lasers," *Opt. Exp.*, vol. 21, no. 7, pp. 8007–8017, Apr. 2013, doi: [10.1364/OE.21.008007](https://doi.org/10.1364/OE.21.008007).
- [15] J. Nürnberg, B. Willenberg, C. R. Phillips, and U. Keller, "Dual-comb ranging with frequency combs from single cavity free-running laser oscillators," *Opt. Exp.*, vol. 29, no. 16, p. 24910, Aug. 2021, doi: [10.1364/oe.428051](https://doi.org/10.1364/oe.428051).
- [16] J. Yu *et al.*, "An airborne $2\text{-}\mu\text{m}$ double-pulsed direct-detection LiDAR instrument for atmospheric CO_2 column measurements," *J. Atmos. Ocean. Technol.*, vol. 34, no. 2, pp. 385–400, Feb. 2017, doi: [10.1175/JTECH-D-16-0112.1](https://doi.org/10.1175/JTECH-D-16-0112.1).
- [17] D. J. H. C. Maas *et al.*, "Vertical integration of ultrafast semiconductor lasers," *Appl. Phys. B, Lasers Opt.*, vol. 88, no. 4, pp. 493–497, Sep. 2007, doi: [10.1007/s00340-007-2760-1](https://doi.org/10.1007/s00340-007-2760-1).